CHAPTER VI
SELF-ASSEMBLY NANOSPHERE INDUCTION VIA CONTROLLED STRUCTURE CHITOSAN

Abstract

Chitosan spheres are obtained directly from the homogeneous reaction of N-phthaloylchitosan and mPEG-COOH. The products provide a stable white colloidal solution in either aqueous or organic solvents. The colloidal particles are sphere in shape with various sizes depending on the chain length and the feed content of mPEG. The spheres obtained from mPEG with M_n = 5000 Dalton show the average sizes about 80-100 nm, whereas those from mPEG with M_n = 550 Dalton show the sizes in the range of 400-500 nm as declared by transmission electron microscopy (TEM) and dynamic light scattering technique (DLS). Chitosan nanospheres show the incorporation with model drug molecule in high stability as seen in the case of stearylamine. The present work originally declares that by simply adjusting the hydrophobic/hydrophilicity of chitosan chain, the self-assembly structure is induced effectively to form spheres in shape with the size of nano-level without any specific processing technique.

Introduction

For the past decades, polymeric materials, both synthetic and biopolymers, as drug carriers for the uses in pharmaceutical[1], medical[2], and agricultural[3] fields have been developed continuously to practical applications. Considering drug delivery system (DDS), the challenge for high efficiency prodrug is about drug incorporation and systematic release mechanism. The drug incorporation can be achieved either by physical processing[4] or by chemical conjugating methods[5]. The processing methods are, for example, film and membrane casting, bead dropping, and gel forming, where the drug molecules are physically incorporated. The prodrug obtained from processing can be easily done; however, the random network of those items limits the systematic controlled release level, and in most cases the uses of crosslinking is also related to the toxicity of the crosslinkers. For chemical conjugating method, drugs are chemically attached to polymer chains via some spacers using specific reactions. Although this method gives a promising release of drugs since it occurs at molecular level, the problems are the risks to lose active sites during the reaction steps between polymer chains and drugs.

Recently, various molecular designs are proposed to obtain effective drug incorporation onto polymer chains in micro/nanoscales since it is an alternative way to avoid the complication of chemical reactions but at the same time achieve the systematic release of drugs. Polymeric spheres are ideal items with a regular size and shape to incorporate drugs via non-covalent bonds i.e., hydrophobic and/or hydrophilic interactions to give prodrugs with a maintained drug active site as well as the high efficiency in controlled release under the high surface area of particles. In general, the key factor for sphere formation is the self-aggregation of amphiphilic polymeric chains in order to minimize the difference in interfacial free energies in aqueous and/or organic solvents[6]. Up to now, there have been reports about the development of nanospheres, for example, Akashi et al.[6] proposed the conjugation of the hydrophilic chains onto polystyrene to obtain core-corona nanospheres, which are further immobilized with peptides for the uses as anti-HIV prodrugs.

Chitosan is a natural aminocopolysaccharide derived from the deacetylation of chitin, which is a component in exoskeleton of crustacean and insects as well as in cell wall of yeasts and fungi. Owing to the unique properties, i.e., biodegradability,[7]

biocompatibility,[8] bioactivity,[9] and non-toxicity,[10] chitin-chitosan is satisfied for the uses in controlled release system in pharmaceutical,[11] biotechnological,[12] and agricultural areas[13]. In the past, many reports and patents show the uses of chitosan in drug delivery system in the forms of films,[14] beads,[15] gels,[16] and membranes[17]obtained from physical processing methods or chemical reaction pathways. Among those reports, there are several touch upon the processing of chitosan spheres in the range of 10~700 μm derived from some specific techniques and conditions such as suspension crosslinking,[18] spray-drying coagulation,[19] and emulsification/solvent evaporation.[20]

Polymeric spheres obtained from chemical reaction were actively studied by Akashi et al.[6] For example, polystyrene-mPEG was prepared as a sphere under the self-assembled core-corona structure. However, until now, there has been no report about the chitosan spheres obtained directly from chemical reaction.

On this viewpoint, in the recent years, we have concentrated on the controlled structured chitosan based on the modification with hydrophobic/hydrophilic groups.[21] We aim to show that a novel type of chitosan nanosphere can be eventually accomplished if the core-corona structure of chitosan is favorable at molecular level under the unique self-assembly structure.

Experimental Section

Materials

Chitosan (degree of deacetylation (DD) = 0.9 and $M_v = 1.7 \times 10^5$ Dalton) was provided by the Seafresh Chitosan (Lab) Company Limited, Thailand. Phthalic and succinic anhydrides were purchased from Fluka Chemika, Switzerland. Poly(ethylene glycol)methyl ethers (mPEG) with the number average molecular weight (M_n) of 550, 2000, and 5000 were obtained from Aldrich Chemical Company, Inc., USA. 1-ethyl-3-(3'-dimethylaminopropyl)carbodiimide (WSCI) was purchased from TCI, Japan. 1-hydroxy-1H-benzotriazole, monohydrate (HOBt) was obtained from BDH Laboratory Supplies, England. *N,N*-Dimethylformamide (DMF) was supplied by UNIVAR, Australia. Hydrazine monohydrate was purchased from Nacalai Tesque Inc., Kyoto, Japan. All chemicals were used

without further purification.

Instruments and Equipment

FT-IR spectra were recorded on a VECTOR 3.0 BRUKER spectrometer with 64 scans at a resolution of 4 cm^{-1} using a deuterated triglycinesulfate detector (DTGS) with a specific detectivity, D^*, of 1×10^9 $cm.Hz^{1/2}w^{-1}$. ^{13}C CP/MAS NMR spectra were taken at 300 MHz with a BRUKER DPX-300 at 23 ± 1°C. ^1H-NMR spectra were obtained from a JEOL GSX 400 (400 MHz) at 70 ± 1°C. Elemental analysis (EA) results were obtained using a YANAKO CHN CORDER MT-3, MT-5 Analyzer with a combustion temperature at 950°C under air with O_2 as a combustion gas (flow rate 20 mL/min) and He as a carrier (flow rate 200 mL/min). A Dupont thermogravimetric analyzer was used for thermal gravimetry analysis (TGA) studies using an N_2 flow rate of 20 mL/min and a heating rate of 20°C/min from 30° to 600° C. Scanning electron microscopy (SEM) analysis of the products was obtained from a JEOL JSM-5200 at an operating voltage of 25 kV. Transmission electron microscopy (TEM) analysis was carried out using a Hitachi H700 at an accelerate voltage of 200 kV. The samples after dialysis in water were casted on a copper mesh and dried under reduced pressure, and subsequently sputtered with carbon 20-50 nm in thickness. Electron spectroscopy for chemical analysis (ESCA) was performed with a Shimadzu ESCA1000 apparatus employing Mg X-ray source (1253.6 eV) and a pass energy of 31.5 eV operating at 8 kV and 20 mA. Powder samples were placed on the Mo plate (15×15 mm^2) by double-side carbon tape, whereas sample solutions were dropped on Mo plate. Dynamic Light Scattering (DLS) measurement was carried on a COULTER® model N4SD at 20°C with the scattering angle 90°.

Procedures

N-Phthaloylchitosan, 2

The preparation of N-phthaloylchitosan was carried out according to published procedure.[21-22] Briefly, chitosan, 1 (1.00 g) was reacted with phthalic anhydride (4.48 g, 5 moles equiv to pyranose rings) in *N,N*-dimethylformamide

(DMF) (20 mL) at 100°C under nitrogen for 6 h. The temperature was reduced to 60°C and the mixture was left overnight. The solution was concentrated and reprecipitated in ice water. The precipitate was collected, washed with ethanol three times, and dried in vacuo to give pale yellow product of **2** (Scheme 1).

Anal. Calcd. for $(C_{14}H_{13}O_6N)_{0.8}(C_6H_{11}O_4N)_{0.1}(C_8H_{13}O_5N)_{0.1}$: (%) C, 56.17; H, 4.75; and N, 5.20. Found: (%) C, 56.18; H, 4.45; and N, 4.35: FT-IR (KBr, cm^{-1}) 3472 (OH), 1776 and 1714 (C=O anhydride), and 721 (aromatic ring): ^{13}C CP/MAS NMR (δ, ppm) 23.3 (CH_3), 57.0 (C-2), 64.7 (C-6), 73.2 (C-3, C-5), 80.5 (C-4), 100.4 (C-1), 131.1 (aromatic ring), and 169.1 (C=O): ^1H-NMR (δ, ppm) 1.7 (CH_3 in acetamide), 3.4-5.0 (pyranose ring), and 7.6-7.7 (aromatic ring).

Poly(Ethylene Glycol) Methyl Ether Terminated Carboxylic Group, 3

Poly(ethylene glycol) methyl ether (mPEG, M_n = 5000 Dalton, 3.00 g, 6×10^{-4} moles) was reacted with succinic anhydride (0.06 g, 1 mole equiv to mPEG) in DMF (2 mL) at 60 °C for overnight with a catalytic amount of pyridine. The mixture solution was extracted by diethyl ether and dried in vacuo to yield white powder of mPEG5000-COOH, **3C** (Scheme 1). Compounds **3A**, and **3B** were similarly prepared but using different molecular weights of mPEG, i.e., 550 and 2000, respectively.

FT-IR (KBr, cm^{-1}) 3472 (OH), 2875 (C-H stretching), 1736 (C=O), and 1105 (C-O-C): ^1H-NMR (δ, ppm) 2.4 (CH_2 in succinic anhydride), 3.2 (O-CH_3), and 3.5 (CH_2 in PEG).

N-Phthaloylchitosan-mPEG-COOH, 4

Compound **3C** (7.58 g, 0.40 moles equiv (40%) to **2C**) was stirred with **2C** (1.00 g, 3.71×10^{-3} moles) in 20 mL of DMF solution containing 1-hydroxy-1H-benzotriazole, monohydrate (HOBt, 0.68 g, 3 moles equiv to **3C**) at room temperature until the solution was clear. 1-Ethyl-3-(3-dimethylaminopropyl)-carbodiimide, hydrochloride (WSC, 0.85 g, 3 moles equiv to **3C**) was added to react at 4°C for 30 min and then room temperature for overnight. The mixture was dialyzed in water for several days before thoroughly washed with methanol and dried

in vacuo to obtain white particles, **4C40** (Scheme 1). A series of the compounds **4C02**, **4C05**, **4C10**, and **4C20** were also prepared by varying the amount of **3C** for 0.02, 0.05, 0.10, and 0.20 moles equiv to **2C**, respectively.

Anal. Calcd. for **4C02**, $(C_{14}H_{13}O_6N)_{0.786}(C_{245}H_{471}O_{122}N)_{0.015}(C_6H_{11}O_4N)_{0.096}$ $(C_{468}H_{927}O_{236}N)_{0.004}(C_8H_{13}O_5N)_{0.098}$ $(C_{239}H_{471}O_{12}N)_{0.002}$: (%) C, 55.65; H, 6.06; and N, 3.60. Found: (%) C, 53.80; H, 4.69; and N, 3.73: Anal. Calcd. for **4C10**, $(C_{14}H_{13}O_6N)_{0.727}(C_{245}H_{471}O_{122}N)_{0.073}(C_6H_{11}O_4N)_{0.082}(C_{468}H_{927}O_{236}N)_{0.018}(C_8H_{13}O_5N)_{0.091}$ $(C_{239}H_{471}O_{12}N)_{0.009}$: (%) C, 55.02; H, 7.69; and N, 1.61. Found: (%) C, 55.04; H, 4.61; and N, 4.47: Anal. Calcd. for **4C20**, $(C_{14}H_{13}O_6N)_{0.655}(C_{245}H_{471}O_{122}N)_{0.146}$ $(C_6H_{11}O_4N)_{0.064}(C_{468}H_{927}O_{236}N)_{0.036}(C_8H_{13}O_5N)_{0.082}(C_{239}H_{471}O_{12}N)_{0.018}$: (%) C, 54.81; H, 8.23; and N, 0.95. Found: (%) C, 55.99; H, 4.73; and N, 5.94: Anal. Calcd. for **4C40**, $(C_{14}H_{13}O_6N)_{0.509}(C_{245}H_{471}O_{122}N)_{0.291}(C_6H_{11}O_4N)_{0.027}$ $(C_{468}H_{927}O_{236}N)_{0.073}(C_8H_{13}O_5N)_{0.064}$ $(C_{239}H_{471}O_{12}N)_{0.036}$: (%) C, 54.67; H, 8.58; and N, 0.52. Found: (%) C, 56.22; H, 4.82; and N, 6.82: Anal. Calcd. for **4A40**, $(C_{14}H_{13}O_6N)_{0.509}(C_{109}H_{199}O_{55}N)_{0.291}(C_6H_{11}O_4N)_{0.027}(C_{196}H_{383}O_{102}N)_{0.073}$ $(C_8H_{13}O_5N)_{0.064}(C_{103}H_{199}O_{54}N)_{0.036}$: (%) C, 54.48; H, 7.95; and N, 1.11. Found: (%) C, 56.39; H, 4.46; and N, 7.21: Anal. Calcd. for **4B40**, $(C_{14}H_{13}O_6N)_{0.509}$ $(C_{107}H_{195}O_{54}N)_{0.291}(C_6H_{11}O_4N)_{0.027}(C_{192}H_{375}O_{100}N)_{0.073}(C_8H_{13}O_5N)_{0.064}$ $(C_{101}H_{195}O_{53}N)_{0.036}$: (%) C, 54.48; H, 7.93; and N, 1.12. Found: (%) C, 56.37; H, 4.40; and N, 7.09: FT-IR (KBr, cm^{-1}) 3464 (OH), 2882 (C-H stretching), 1776 and 1714 (C=O anhydride), 1714 (C=O ester), and 721 (aromatic ring): ^{1}H-NMR (δ, ppm) 2.4 (CH_2 in succinic anhydride), 3.2 (O-CH_3), 3.5 (CH_2 in PEG), 2.8-4.7 (pyranose ring), and 7.6-7.8 (aromatic ring).

Chitosan-mPEG-COOH, 5

Compound **4C40** (1 g) was stirred in DMF (10 mL) at 90°C under nitrogen atmosphere for 1 h. Hydrazine monohydrate was added and the reaction was continued for 2 h. The mixture was reprecipitated in acetone and the obtained precipitate was washed thoroughly by methanol before dried in vacuo to give **5C40** (Scheme 1).

FT-IR (KBr, cm^{-1}) 3412 (OH), 2882 (C-H stretching), 1714 (C=O ester), 1654 (amide I), 1549 (amide II), and 895 (pyranose ring): ^{1}H-NMR (δ, ppm) 1.8 (CH_3 in acetamide), 2.4 (CH_2 in succinic anhydride), 2.9 (O-CH_3), 3.3 (CH_2 in PEG), 3.2-5.0 (pyranose ring), and 7.6-7.7 (aromatic ring).

Model Molecule Incorporation

Stearylamine in isopropanol was prepared (0.02 mol/l). Compound **4C40** (0.15 g) was sonicated in isopropanol (5 mL) for few minutes before adding 5 mL of stearylamine-isopropanol solution. The mixture was slightly stirred for overnight. The precipitate was collected and re-dispersed in water. The white powder was kept and washed thoroughly with water and methanol before drying in vacuo.

Results and Discussion

Synthesis and Structural Characterization

Compound 2

Phthalic anhydride was introduced onto chitosan chain not only as an amino protecting group but also as a bulky group to improve the solubility of chitosan. Figure 1 clarifies that **2** shows new peaks of the phthalimido group at 1776 and 1714 cm^{-1} referring to carbonyl anhydride and 721 cm^{-1} belonging to aromatic ring (Figure 1(d)). ^{13}C CP/MAS NMR pointed out the aromatic ring in phthalimido group as a single sharp peak at 131.1 ppm, and two types of C=O belonging to acetamide and phthalimido groups at 169.1 ppm. In addition, ^{1}H-NMR also supported the successful phthaloylation as seen from the peak at 7.6 ppm belonging to protons of the phenyl ring. The degree of N-phthaloylation was 89 % as evaluated by elemental analysis. From these results, it was concluded that the phthalimido group was successfully introduced onto chitosan. It was found that compound **2** was easy to dissolve in organic solvents such as DMF, dimethyl sulfoxide (DMSO), dimethylacetamide (DMAc) and pyridine. This provides the homogeneous systems for chemical modification in the following step.

Compound 3

Here, mPEG was terminated with hydroxyl group by reacting with succinic anhydride to obtain **3**. Compound **3** shows the peak at 2875 cm^{-1} belonging to methylene group, 1736 cm^{-1} for carbonyl, and 1105 cm^{-1} for ether bond (C-O-C) (Figure 1(b)). ^1H NMR also confirmed the successful of the reaction as seen from new peak at 2.4 ppm possessing to methylene protons in succinic anhydride.

Compound 4

Compounds **2** and **3** were reacted in homogeneous system and the solution obtained was dialyzed for several days to obtain white precipitate of **4**. Compound **4** shows the increase in peak intensity at 2882 cm^{-1} belonging to methylene groups implying the conjugation with mPEG is successful (Figure 1(e)). ^1H NMR also supported the mPEG conjugation as seen from the peaks at 2.4, 3.2, and 3.5 ppm referring to methylene protons of succinic anhydride, methoxy protons of mPEG terminal chain, and methylene protons of mPEG, respectively.

Here, EA was applied to evaluate mPEG substitution onto phthaloylchitosan. For example, in the case of mPEG with M_n 5000, percent substitution of **3C02**, **3C10**, **3C20**, and **3C40** are 93, 36, 16, and 8, respectively (Table 1). The mole substitution was then calculated to be 0.0187, 0.0360, 0.0327, and 0.0316, respectively, to find the saturating substitution at about 0.03. It is important to note that when the feed content of **3** increases, the reaction efficiency decreases. This might be due to the significant chain-chain interaction among **3** in high concentration to restrict the chain mobility in the reaction. In addition, when we controlled the feed content of **3** (0.40 moles) but varied M_n of mPEG (550, 2000, and 5000), we found the shorter the mPEG chain length, the higher the % substitution of **3** on **2** (Table 1). This also supported our speculation about chain mobility.

Compound 5

In order to confirm that the balance of hydrophobic/hydrophilicity brings the assembly structure to chitosan, an attempt to remove phthalimido group was done. Figure 1(f) shows FT-IR spectrum of compound **5** to find that the peaks at 1776 and 721 cm^{-1} belonging to C=O in anhydride and benzene ring, respectively disappeared,

whereas the peak intensity of C=O at 1714 cm^{-1} decreased. This implied the successful deprotection. Compound **5** was also used to study the colloidal phenomena and the nanospheres formation.

Colloidal Formation and Effect of Solvents

Generally, chitosan and most of its derivatives are insoluble and difficult to disperse in water and common organic solvents as shown in Figure 2(A)(a). Compound **2** shows some turbidity in water after sonication (Figure 2(A)(b)), which implies the tendency to form micelle-like structure. This might be due to the self-aggregation of hydrophobic phthalimido groups on chitosan chain.

After chitosan was conjugated with mPEG to obtain **4**, a series of colloidal phenomena in various solvents were observed. Figure 2(B) shows the colloidal solution of **4** in protic and aprotic solvents, i.e., water, 1% aqueous acetic acid, methanol, ethanol, iso-propanol, DMF, DMSO, chloroform, toluene, and hexane. The solvents were selected based on the variation of dielectric constant and dipole moment to observe the colloidal induction by the solvent molecules. In the cases of protic solvents (i.e., water, 1% acetic acid, methanol, ethanol, and iso-propanol), the turbidity was clearly observed (Figure 2(B)(a)-(e)). For aprotic solvents (i.e., DMF, DMSO, toluene, n-hexane, chloroform), it is important to note that **4** is completely dissolved in DMF and DMSO (Figure 2(B)(g)-(h)); however, it is insoluble in toluene and n-hexane (Figure 2(B)(i)-(j)). This might be related to the dielectric constant and dipole moment of DMF and DMSO (Table 2).

In the cases of protic solvents, we speculated that the colloidal phenomena were induced via the hydrogen bond. Scheme 2(a) illustrated the water system of **4**, which the hydrogen bonds are formed between solvent molecules and mPEG chains of **4**, whereas N-phthalimido group acts as a hydrophobic segment. It is important to note that the milky solution is stable for more than a week at ambient. The stability of **4** might come from the steric hindrance of mPEG chains, which are sticking out and repulsing each other. In the cases of aprotic solvents, as shown in Scheme 2(b), the complete dissolvation of **4** in DMSO might occur under ionic interaction between solvent molecules (δ^+ at sulfur atoms) and chitosan at both mPEG chains and phthalimido groups (δ^- at oxygen atoms). For n-hexane and

toluene, the precipitation of **4** might result from the lack of solute-solvent interactions. It is important to note that **4** forms colloidal solution in chloroform (Figure 2(B)(f)). This might come from the fact that the dipole moment of chloroform compensates the dielectric constant value and induces the partially ionic interaction with **4**.

At this stage, we concluded that the hydrophilicity and hydrophobicity on the chain at a certain level induced the colloidal formation whereas the apparent turbidity was related to the preferable solvent-chitosan structure. It should be noted that when phthalimido groups were removed (compound **5**), the colloidal phenomena could not be observed in any solvent as shown in Figure 2(C). The particles are not dissolved in any solvent except acetic acid, which might be due to the protonation of amino groups and the hydrogen bonds between water molecules and mPEG chains (Figure 2(D)(a)).

Nanosphere Formation and Effect of Hydrophobic/Hydrophilicity on Shape and Size

Figure 3 shows SEM photographs of chitosan and its derivatives. It was found that **1** shows irregular flake (Figure 3(A)), while **2** performs partially round in shape (Figure 3(B)). The appearance of **2** implied the initial step of sphere formation as a result of phthalimido groups in chitosan chain. Figure 3(C)-(E) confirms that the well-defined spheres are existed in the colloidal solution obtained from various solvents. The sizes of chitosan spheres were varied from few micrometers to hundred nanometers. For example, the sizes were averagely observed to be 200 nm for **4C40** (Figure 3(C) and (D)) and 2 μm for **4B40** (Figure 3(E)). It should be noted that **5** loses the sphere-like structure to be flake-like one as shown in Figure 3(F). In order to reveal the information about individual sphere and/or its primary structure, TEM was applied. Figure 4 illustrates TEM photographs of **4**, the images of **4** confirm the round shape particle with different sizes. It was found that the sizes of **4A40** (Figure 4(A)), **4C02** (Figure 4(B)), and **4C40** (Figure 4(C)) are 400, 165, and 85 nm, respectively. Serizawa et al.[23] reported that the small size of polystyrene-mPEG core-corona nanospheres was induced by the long mPEG chain. For the present work, we speculate the similar

structure which chitosan moiety acts as a core and mPEG chain as a corona. The size of the nanospheres, thus, should be related to the chain length and the feed content of mPEG. Here, DLS was further applied to confirm the effect of mPEG chain length and its feed content in controlling the size of nanospheres. Figure 5(A) illustrates the M_n of **3**, whereas Figure 5(B) shows the feed content affected on the sphere size to find that these factors control the size of sphere. Figure 5 shows the sphere sizes are in average of 300-600 nm.

Information of Nanosphere Surface

As shown in Scheme 2, we speculated that the colloidal phenomena and sphere formation were induced under the self-assembly mechanism when the molecule consists of hydrophobic and hydrophilic parts. E SCA was carried out to determine the functional group on the sphere surface. Figure 6 shows the surface energy in the modes of C_{1s}, N_{1s}, and O_{1s} of compounds **1**, **2**, **3**, and **4**. C ompounds **1**, **2**, and **3** were used as references (Figure 6(a)-(c)), whereas two types of **4**, i.e., without treating in solvent (Figure 6(d)) and with treating in solvents (water, iso-propanol, chloroform, and toluene) (Figure 6(e-h)), were used for comparative studies.

In the cases of **1** and **2**, the binding energy of N_{1s} was 401.8 eV referring to the functional groups C-N, O=C-N, and O=C-N-C=O, implying chitosan and N-phthaloylchitosan on the surface. It is natural to find that **3** provided no N_{1s} peak as it is mPEG. C omparing to **4**, compounds **1**-**3** gave higher binding energy, especially in the case of O_{1s} (Figure 6(C)(a)-(c)). This might be due to the fact that each compound (**1**-**3**) is long chain polymer aligned in regular manner. H owever, in the case of **2** (Figure 6(C)(b), since the bulky phthalimido groups were conjugated onto the chain to obstruct the inter- and intra-molecular hydrogen bonds, as a result, the binding energy (534.5 eV) is lower than that of **1** (535.2 eV). C onsidering **4C40** in dry solid s tate (Figure 6 (B)(d)) a nd **4 C40** after dispersing i n i so-propanol (Figure 6(B)(f)), the peak cover wide ranges of binding energies at around 535.2 eV implying that the C-O-H of chitosan, N-C=O of phthalimido group, and C-O-C of mPEG chain were randomly existed on the surface of spheres.

In chloroform (Figure 6(B)(g)), the sphere surface shows phthalimido group and mPEG as clarified from two species of O_{1s} at 530.4 and 532.5 eV, referring to

oxygen atoms of mPEG and phthalimido group, respectively. This result was relevant to colloidal formation phenomena (Figure 2(B)(f)).

When toluene was used as medium, the colloidal formation was not observed (Figure 2(B)(i)). Here, the sphere surface after treating with toluene gave a significant peak of O_{1s} at 530.4 eV referring to mPEG and a minor peak at 533.5 eV belonging to phthalimido group (Figure 6(B)(h)) implying that the interaction of **4** with toluene was rather difficult. For spheres after dispersing in water, the result declared that the sphere surface mainly consisted of mPEG as identified from the peak of O_{1s} at 531.2 eV belonging to O-C=O, C-O-C, and C-O-C=O of mPEG (Figure 6(B)(e)).

The observation under N_{1s} mode was further studied to find that all of **4C40** gave the peak at 402.0 eV referring to C-N-H of amino and acetamide groups of chitosan. This suggested that the sphere surface covered with chitosan unit. However, **4C40** after dispersing in chloroform and toluene showed the peak at 398.3 eV for phthalimido group implying that those solvents partially induced the phthalimido group on the surface. In conclusion, the self-assembly of chitosan was induced by solvents; as a result, colloidal phenomena was formed. Water molecule might initiate preferable molecular assembly, thus, it gives high stable milky solution.

Model drug Incorporation

It is important to clarify how we can apply chitosan sphere as a novel material for polymeric prodrug. Here, drug conjugation is done in three steps: (i) dispersing spheres in iso-propanol to allow some hydrophobic aligning on the surface, (ii) mixing with stearylamine model drug, and (iii) collecting the spheres and re-dispersing in water. By those steps, we assured that stearylamine was incorporated by hydrophobic-hydrophobic interaction at molecular level. Drug conjugation was succeeded as confirmed by FT-IR at 2878 cm^{-1} (Figure 7). Thermogravimetric analysis indicated the degradation temperature of stearylamine at 310°C (Figure 8) and percent incorporation to be 15.4.

Conclusion

The present work demonstrated that by grafting hydrophilic chains, mPEG, to hydrophobic polymer, N-phthaloylchitosan, we could obtained sphere particles directly from the reaction without specific processing technique. Colloidal phenomena and nanosphere formation were induced by the polarity of the media. The chain length and the feed content of hydrophilic mPEG chains were the factors to control the sphere sizes. The chitosan nanospheres showed the drug incorporation as identified from the model case of stearylamine.

Acknowledgements

The authors would like to thank Seafresh Chitosan (Lab) Company Limited, Thailand for providing the chitosan starting material. The authors are grateful to Prof. Seiichi Tokura (Kansai University, Japan) for useful discussions, suggestions, and comments. The authors are indebted to the Rigaku International Corporation, Japan and the Hitachi Scholarship Foundation, Japan for partially financial support. Appreciation is expressed to National Science and Technology Development Agency of Thailand, National Metal and Materials Technology Center (MTEC). One of the authors (R.Y.) acknowledges Assoc. Prof. Takeshi Serizawa and Dr. Tatsuo Kaneko (Kagoshima University, Japan) for their suggestions.

References

1. Vandamme, Th. F.; Lenourry, A.; Charrueau, C.; Chaumeil, J-C. *Carbohydrate Polymers* **2002**, *48(3)*, 219-231.
2. Jones, M-C.; Leroux, J-C. *European Journal of Pharmaceutics and Biopharmaceutics* **1999**, *48(2)*, 101-111.
3. Kidchob, T.; Kimura, S.; Imanishi, Y. *Journal of Controlled Release* **1998**, *51(2-3)*, 241-248.
4. Luftensteiner, C.P.; Viernstein, H. *International Journal of Pharmaceutics* **1998**, *171(1)*, 87-99.
5. Oh, J.E.; Nam, Y.S.; Lee, K.H.; Park, T.G. *Journal of Controlled Release* **1999**, *57(3)*, 269-280.

6. Akashi, M.; Niikawa, T.; Serizawa, T.; Hayakawa, T.; Baba, M. *Bioconjugate Chemistry* **1998**, *9*, 50-53.
7. (a)Yamamoto, H.; Amaike, M. *Macromolecules* **1997**, *30*, 3936-3937. (b) Tomihata, K.; Ikada, Y. *Biomaterials* **1997**, *18*, 567-575.
8. (a) Richardson, S.C.; Kolbe, H.V.; Duncan, R. *Int. J. Pharm.* **1999**, *178 (2)*, 231-243. (b) Risbud, M.V.; Bhonde, R.R. *Drug Delivery* **2000**, *7(2)*, 69-75.
9. (a) Matsuhashi, S.; Kume, T.J. *Sci. Food Agric.* **1997**, *73*, 237-241. (b) Dumitriu, S.; Popa, M.I .; Cringu, A.; Stratone, A. *Colliod Polym. Sci.* **1989**, *267*, 595-599.
10. Chandy, T.; Sharma, C.P. *Biomaterials* **1992**, *13(13)*, 949-952.
11. (a) Ohya, Y.; Takei, T.; Ouchi, T. *J Bioact Compat Polym* **1992**, *7*, 243. (b) Ohya, Y.; Takei, T.; Kobayashi, H.; Ouchi, T. *J Microencapsulation* **1993**, *10*, 1.
12. Braun, J.; Le, C.P.; Le, G.F. *Biotechnol. Bioeng.* **1989**, *33(2)*, 242-246.
13. Teixeira, M.; Paterson, W.P.; Dunn, E.J.; Li, Q.; Hunter, B.K.; Goosen, M.F.A. *Ind. Eng. Chem. Res.* **1990**, *29*, 1205-1209.
14. Remuñán-López, C.; Portero, A.; Vila-Jato, J.L.; Alonso, M.J. *Journal of Controlled Release* **1998**, *55(2-3)*, 143-152.
15. Aral, C.; Akbuga, J. *International Journal of Pharmaceutics* **1998**, 168(1), 9-15.
16. Ramanathan, S.; Block, L.H. *Journal of Controlled Release* **2001**, 70(1-2), 109-123.
17. Thacharodi, D.; Rao, K.P. *Biomaterials* **1995**, *16(2)*, 145-148.
18. Denkbas, E.; Odabasi, M.J. *J. Appl. Polym. Sci.* **2000**, *76*, 1637-1643.
19. Mi, F.; Wong, T.; Shyu, S.; Chang, S.J. *J. Appl. Polym. Sci.* **1999**, *71*, 747-759.
20. Genta, I.; Perugini, P.; Conti, B.; Parranetto, F. *International Journal of Pharmaceutics* **1997**, *152*, 237-246.
21. Yoksan, R.; Akashi, M.; Biramontri, S.; Chirachanchai, S. *Biomacromolecules* **2001**, *2*, 1038-1044.
22. Nishimura, S.I.; Kohgo, O.; Kurita, K. *Macromolecules* **1991**, *24*, 4745-4748.
23. Serizawa, T.; Takehara, S.; Akashi, M. *Macromolecules* **2000**, *33*, 1759-1764.

Scheme Captions

Scheme 1. Preparation route of chitosan derivatives: chitosan (**1**), N-phthaloylchitosan (**2**), mPEG-COOH (**3**), N-phthaloylchitosan grafted mPEG (**4**), and chitosan grafted mPEG (**5**)

Scheme 2. Interaction of **4** with protic and aprotic solvents

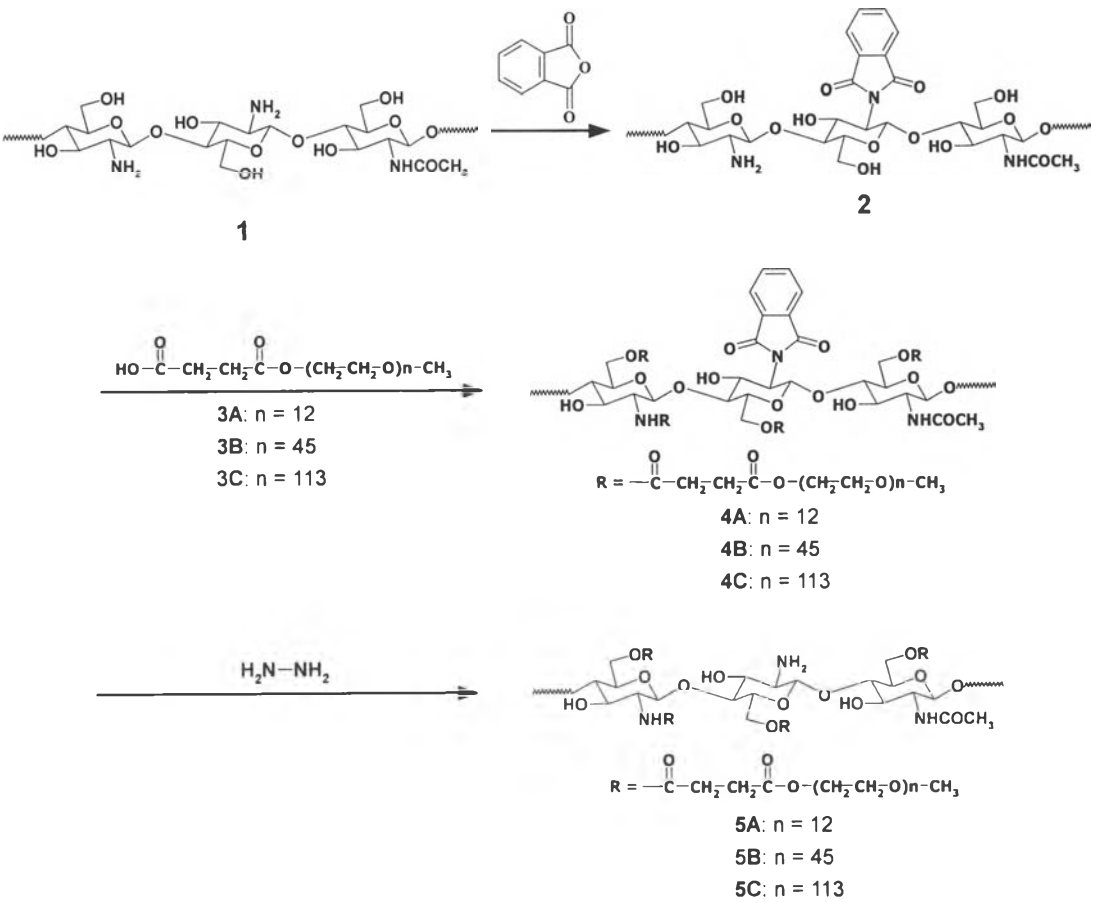

Scheme 1. (Yoksan et al.)

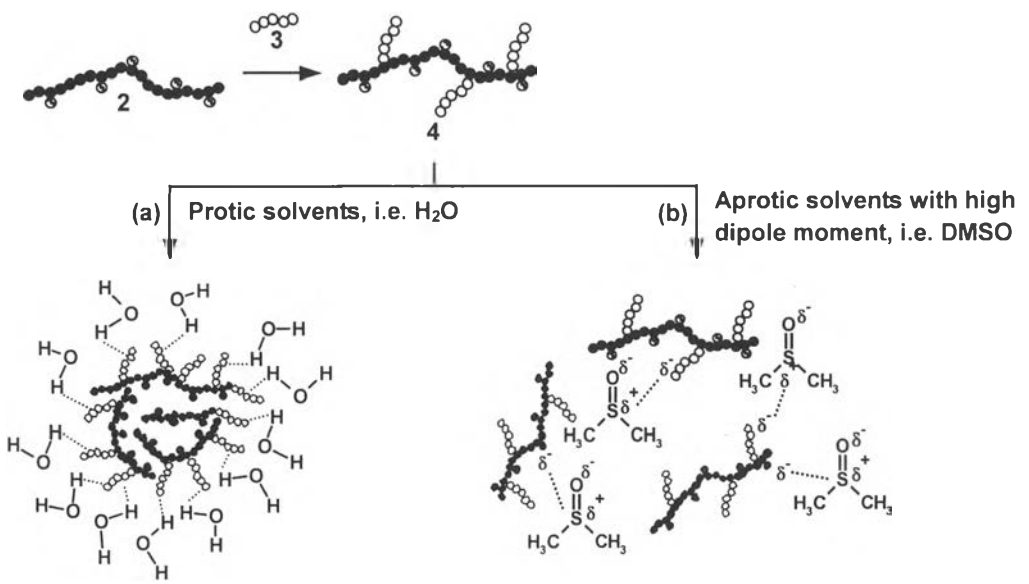

Scheme 2. (Yoksan et al.)

Figure Captions

Figure 1. FT IR spectra of (a) mPEG (M_n = 2000), (b) **3B**, (c) **1**, (d) **2**, (e) **4B40**, and (f) **5B40**.

Figure 2. Appearance of (A) (a), compound **1** in water; (b), compound **2** in water; and (c), compound **4C40** in water, (B) compound **4C40** in (a), water; (b), 1% aqueous acetic acid; (c), methanol; (d), ethanol; (e), iso-propanol; (f), chloroform; (g), DMSO; (h), DMF; (i), toluene; and (j), n-hexane, (C) compound **5C40** in (a), water; (b), 1% aqueous acetic acid; (c), methanol; (d), ethanol; (e), iso-propanol; (f), chloroform; (g), DMSO; (h), DMF; (i), toluene; and (j), n-hexane, and (D) (a) compound **5C40** in1% aqueous acetic acid and (b) compound **4C40** in1% aqueous acetic acid.

Figure 3. SEM photographs at 25 kV of (A) **1** (15,000×), (B) **2** (20,000×), (C) **4C40** (20,000×), (D) **4C40** (50,000×), (E) **4B40** (35,000×), and (F) **5C40** (20,000×).

Figure 4. TEM photographs at 30,000× of (A) **4A40**, (B) **4C02**, and (C) **4C40**.

Figure 5. Size of (A) **4** as a function of M_n of mPEG (feed content of **3** = 0.40 moles) and (B) **4C** as a function of feed content of **3C**.

Figure 6. ESCA spectra of (A) C_{1s}, (B) N_{1s}, and (C) O_{1s} of (a) **1**, (b) **2**, (c) mPEG, (d) **4C40** in dry solid state, (e) **4C40** after dispersing in water, (f) **4C40** after dispersing in iso-propanol, (g) **4C40** after dispersing in chloroform, and (h) **4C40** after dispersing in toluene.

Figure 7. FT IR spectra of (a) **4C40** and (b) **4C40** after stearylamine incorporation.

Figure 8. TGA thermograms of (a) **4C40** and (b) **4C40** after stearylamine incorporation.

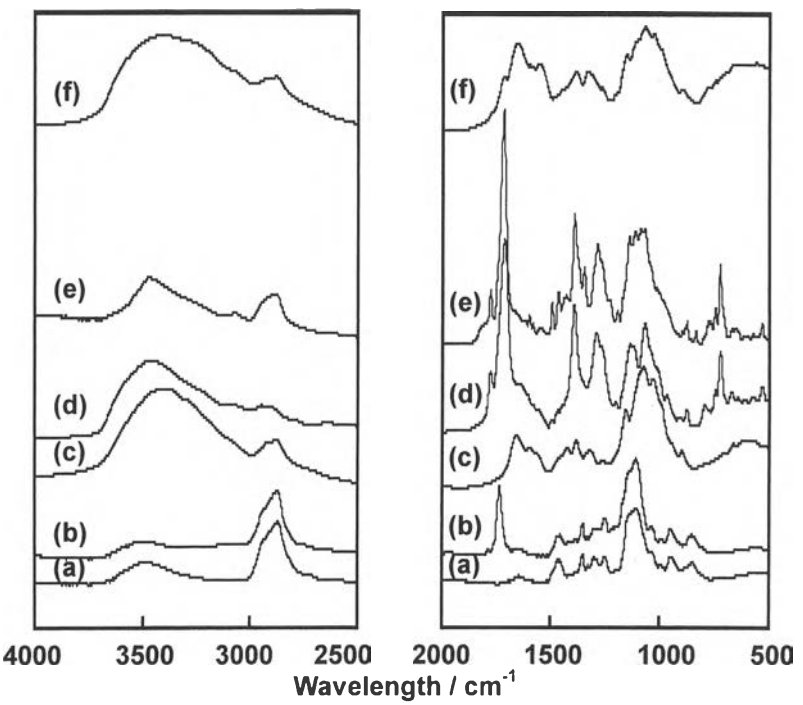

Figure 1. (Yoksan et al.)

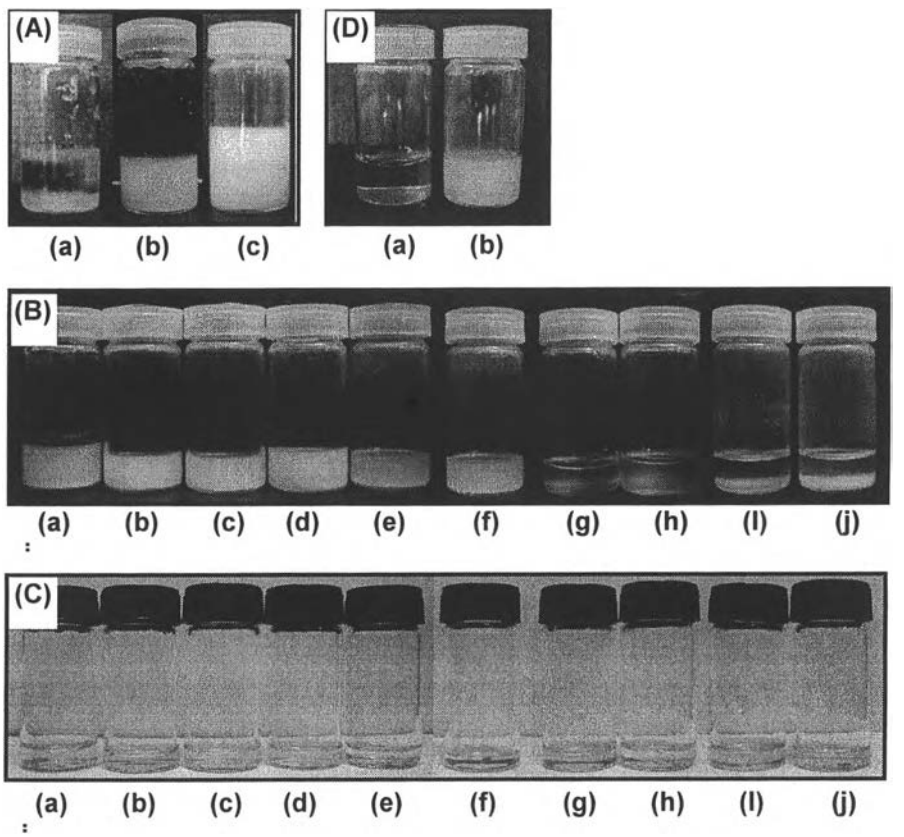

Figure 2. (Yoksan et al.)

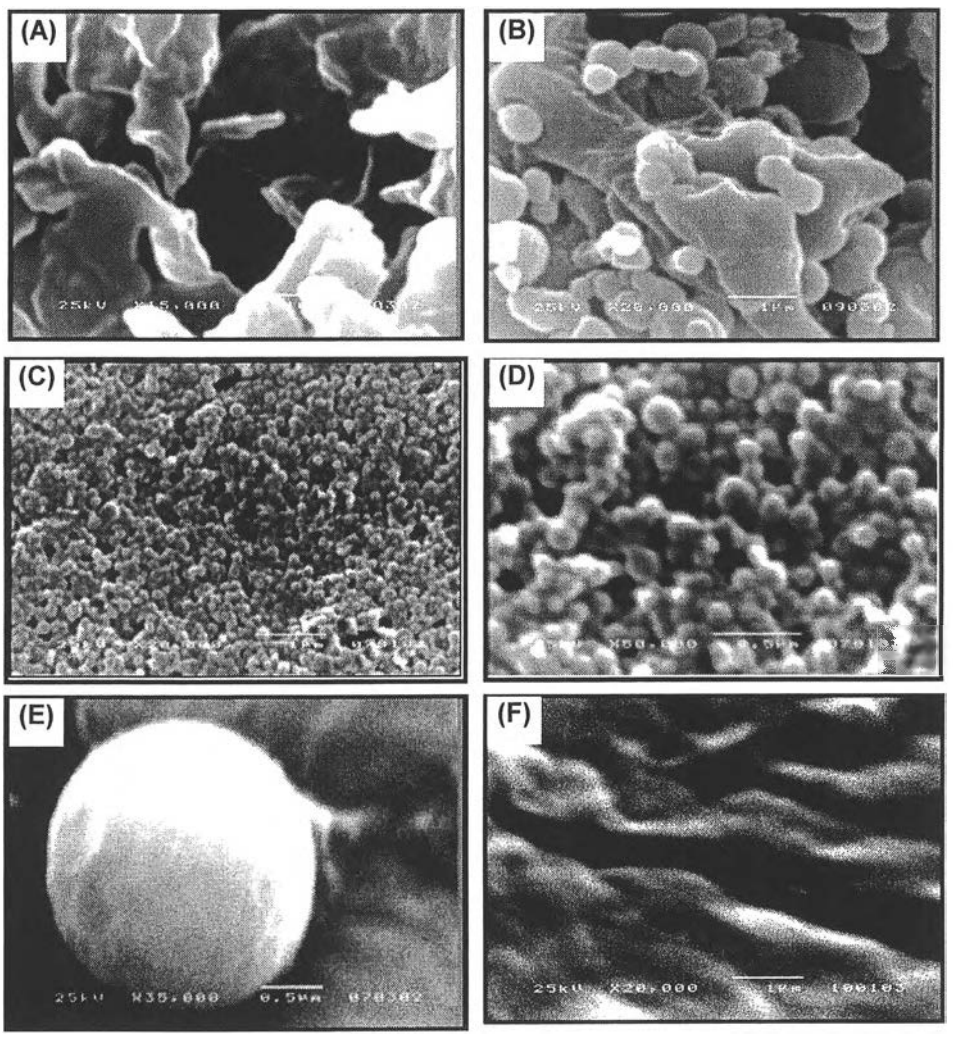

Figure 3. (Yoksan et al.)

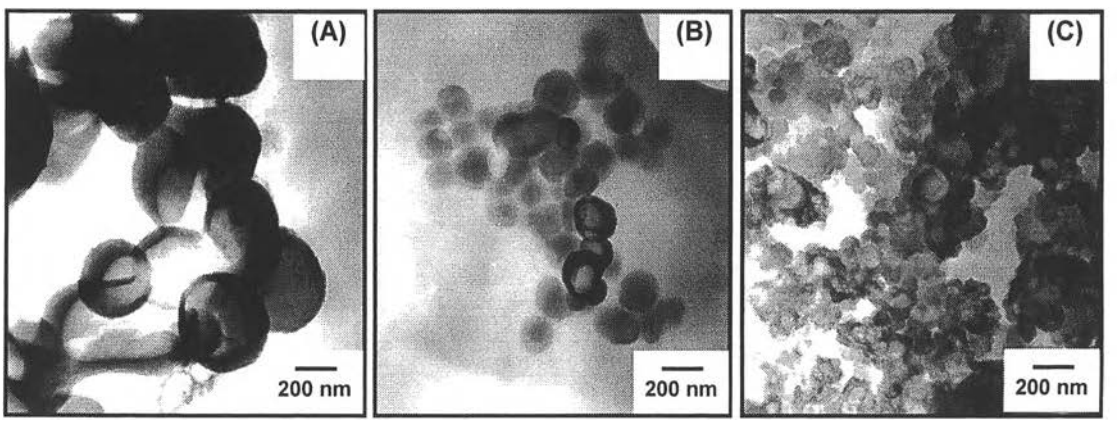

Figure 4. (Yoksan et al.)

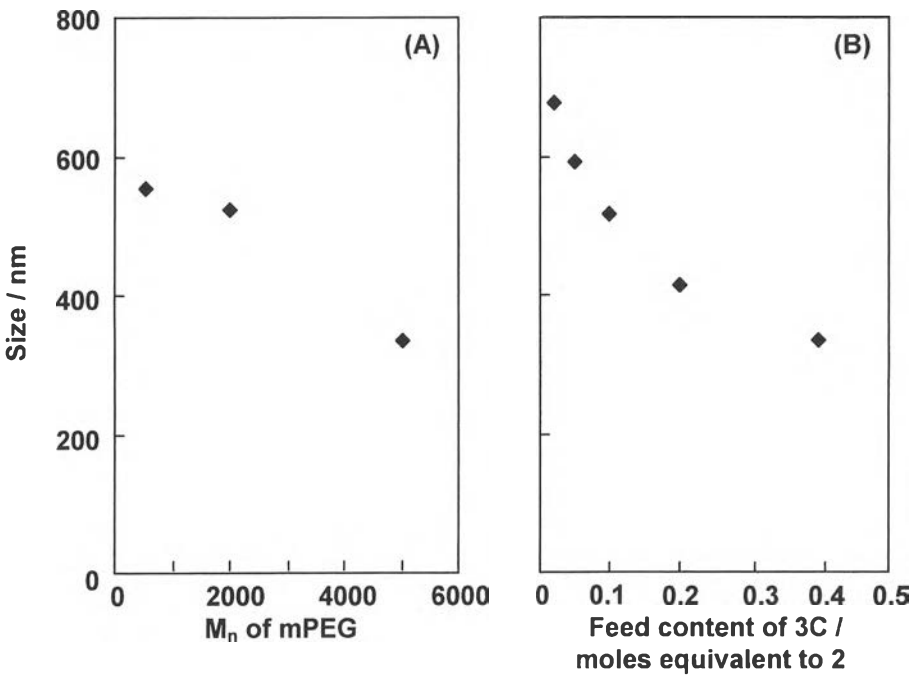

Figure 5. (Yoksan et al.)

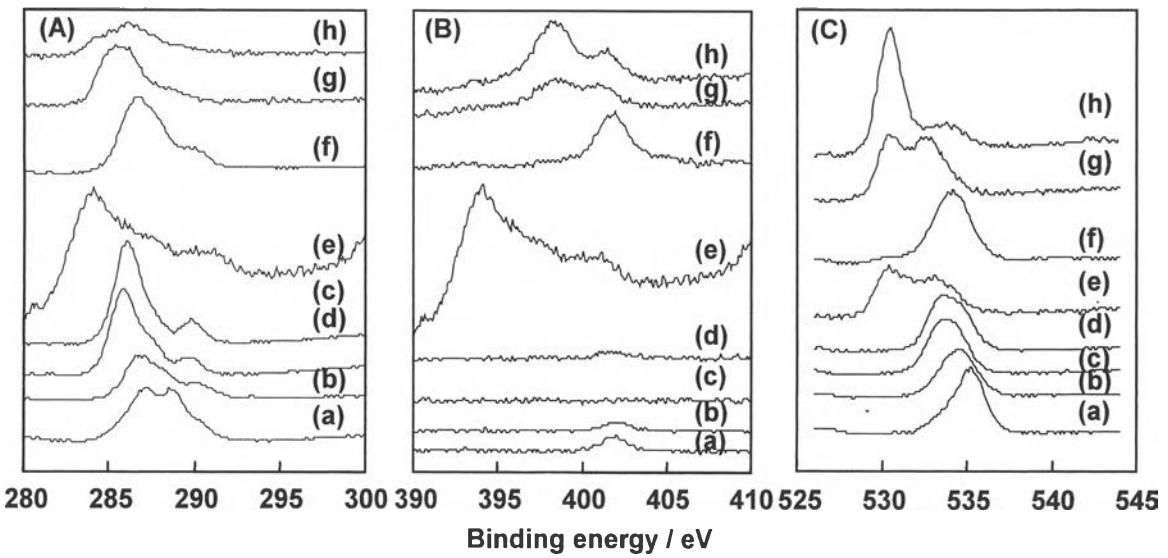

Figure 6. (Yoksan et al.)

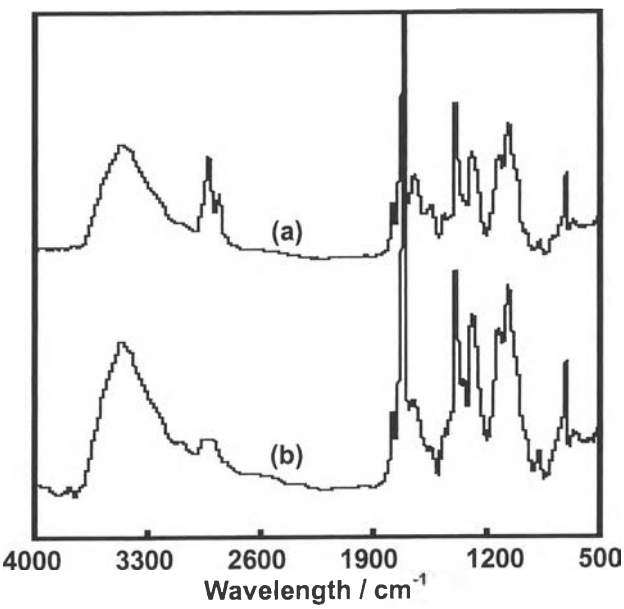

Figure 7. (Yoksan et al.)

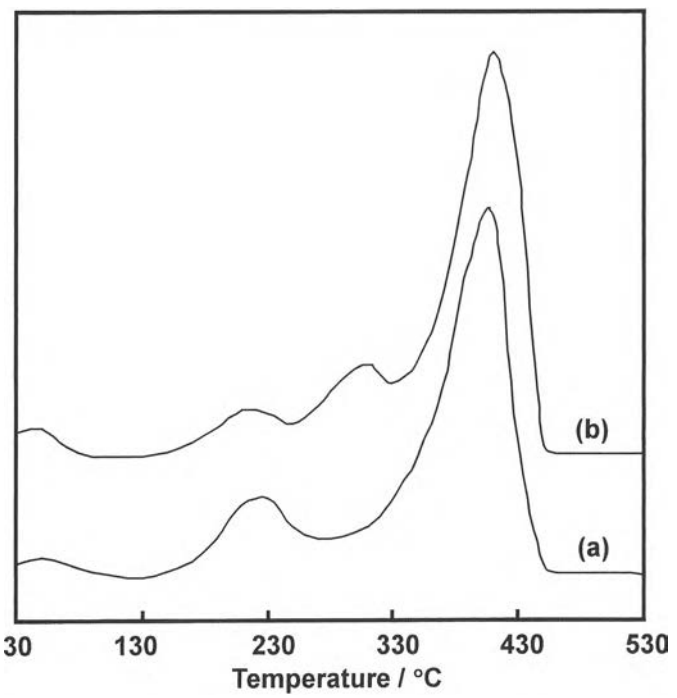

Figure 8. (Yoksan et al.)

Table Captions

Table 1. Percent substitution and mole substitution of **3** on **2**

Table 2. Evaluation of colloidal formation of **4C40** and **5C40** in various solvents relating to dielectric constant and dipole moment

Samples	Mole in feed of **3**	% Substitution of **3**	Mole substitution of **3**
4C02	0.02	93.3	0.0187
4C10	0.10	36.0	0.0360
4C20	0.20	16.0	0.0327
4C40	0.40	7.9	0.0316
4A40	0.40	16.4	0.0654
4B40	0.40	16.0	0.0637

Table 1. (Yoksan et al.)

Solvents	Dielectric constant[b] at 25 °C / Debye	Dipole moment[b] / Debye	Appearance[c]	
			4C40	**5C40**
Water	78.54	1.85	±	-
1% Aq. acetic acid	-	-	±	+
Methanol	32.63	1.70	±	-
Ethanol	24.30	1.69	±	-
Iso-propanol	15.80	1.58	±	-
Chloroform	4.81	1.04	±	-
DMSO	47.00	3.96	+	-
DMF	36.70	3.82	+	-
Toluene	2.38	0.38	-	-
n-Hexane	1.89	0.08	-	-

[a] Brandrup J, Immergut EH (eds) Polymer Handbook, Volume 2, 3rd edn. John Wiley & Sons, USA, pp VII 519

[b] Lide DR (eds) Handbook of Chemistry and Physics, 72nd edn. CRC Press, USA, pp 8-51, 8-49, and 9-18 - 9-26

[c] ±, Colloidal formation; +, Solvation; –, Precipitation

Table 2. (Yoksan et al.)